CORROSION SCIENCE AND TECHNOLOGY, Vol.2, No.1(2003), pp.12~17

Electronic Behaviors of Passive Films Formed on Fe-Cr and Fe-Cr-Mo Ferritic Stainless Steels Studied by Mott-Schottky and Cyclic Voltammetry Techniques

Suk-Won Kim, Sang-In Yoon, and Jae-Bong Lee

School of Metallurgy and Materials Engineering, Kookmin University
861-1 Jeongneung-dong, Sungbuk-ku, Seoul 136-702, Korea

The effects of Cr content and film formation potential on electronic behaviors of the passive film on Fe-Cr alloys were investigated in borate buffer solution. Influence of pH on passive films of both Fe-Cr and Fe-Cr-Mo alloys was also investigated. Mott-Schottky and cyclic voltammetry techniques were used to elucidate electronic behaviors of passive films and their electrochemical characteristics. AES analysis of passive films was carried out. Results showed that doping density decreased as Cr content and film formation potentials increased. The addition of Mo to Fe-Cr alloy had little influence on donor densities in pH 9.2 solution but some effects on the decrease in donor densities in pH 1.6 acidic solution.

Keywords *: mott-schottky, cyclic voltammetry, aes, passive film, stainless steel.*

1. Introduction

Stainless steels have the excellent corrosion resistance, due to the existence of thin passive film which prevents metals from reacting with corrosive environments. The structure, composition and growth process of passive film have been a challenging topic among corrosion scientists. Recently, it was claimed that the electronic structures of the passive film formed on stainless steels were closely related to corrosion resistance[1)-5)] and electrochemical behaviors of passive films were also associated with their properties.[6)-7)]

In order to study electronic properties of passive films, Mott-Schottky plots were used by capacitance measurements.[4)-5),8)-12)] Paola et al.[8)-9)] suggested that passive films on both stainless steel and pure Fe may be amorphous semiconductors through the hysteresis testing of their capacitances with applied potental.

When potentials were applied on passive film contacted with electrolytes, electrochemical potentials were changed at electrolyte/passive film interface, finally causing the change of space charge layer thickness inside of passive film.

In this study, with the change of Cr content and film formation potential, the electronic properties of passive film formed on Fe-Cr alloy were investigated by using Mott-Schottky plot. The chemical reactions occured were identified by cyclic voltammetry technique. AES analysis was also carried out to examine the quantitative chemical composition of the passive film layers. The effects of pH on electronic properties of passive films on Fe-Cr and Fe-Cr-Mo alloys were investigated. The role of alloying element, Mo was examined with regared to the stability of passive films.

2. Experimental

Fe- x Cr (x=0. 18. 25. 30. 40 and 100 wt%) and Fe-18%Cr-4%Mo alloys were made by vacuum arc melting. pH 9.2 buffer solution was prepared with distilled water, H_3BO_3(0.05M) and $Na_2B_4O_7 \cdot 10H_2O$(0.075M). The solution was deaerated with high purity Ar during testing. A very high density graphite and a saturated calomel electrode (sce) were used as counter and reference electrodes, respectively. In order to investigate effects of pH on electronic properties of passive film, in addition to pH 9.2 buffer solution, pH4.7 buffer solution (0.5M CH_3COOH +0.5M CH_3COONa) and pH 1.6 acid solution (0.1N H_2SO_4) were also prepared.

Potentiodynamic polarization experiments were performed on specimens at a scan rate of 1mV/s. Before capacitance tests, specimens were cathodically prepolarized at -1.5V_{sce} for 10min for cleansing, and then polarized for 2 hours at the film formation potentials (0.8?-0.2 V_{sce})for the passive film formation. Capacitance measurements were performed at 1580Hz by using a

potentiostat(Gamry Model CMS105B) and a lock-in amplifier (Gamry SR810, double phase sensitive detector) with electrochemical impedance software (Gamry CMS300). The polarization was applied by successive steps of 50 mV, starting at the film formation potential in the cathodic direction.

Cyclic polarization experiments were carried out on specimens at the scan rate of 50 mV/s from -1.2V_{sce} to the film formation potentials, by using a WBCS battery cycler system controlled by a computer software.

In order to determine the depth profiles of the constitutive elements from solution/film interface to film/metal interface, AES analysis was carried out on specimens at sputter rate of 1.5nm/min.

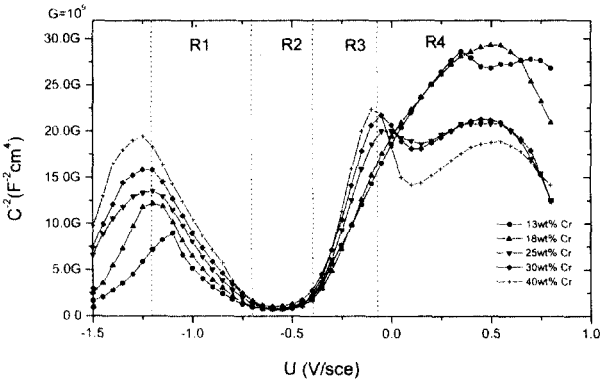

Fig. 1. Plot of 1/C2 vs. the applied potential E for passive film formed at 0.8Vsce on Fe-Cr alloys with various Cr content.

3. Results

3.1 Capacitance measurement results (Mott-Schottky approach)

Fig. 1 shows Mott-Schottky plot of passive films formed on pure Cr and Fe-Cr alloys with various Cr contents. The existence of four potential regions (R1-R4) was also observed, due to different capacitance behaviors with applied potentials, as reported by Hakiki et al..[11] According to Hakiki et al., Cr promotes a p-type semiconductor of Cr oxide layer in the inner part of the passive film, which is in series with an n-type semiconductor layer of iron oxide in the outer part of the film, forming a p-n heterojuntion. The negative (R1) and positive slopes (R3) in Fig. 1 indicate that the passive films behave as p-type and n-type semiconductors, respectively. The complicated behaviors of capacitance in R4 region has been explained by surface roughness and nonuniform donor distribution,[13] or the presence of surface states which alter the potential difference across the Helmholtz layer,[14] or the existence of a second donor level in the band gap that is not ionized at the flat band potential. Regions R1 and R3 are separated by region R3 in which the oxides are in a flat band condition. It appears that as Cr content increases, the slopes of the straight lines of R1 and R3 region increase. However, the increasing width of slope of R1 region was larger than that of R3 region, respectively. Region 4, the capacitance behavior becomes more complicated as Cr content increases. It appears that Fe-13%Cr and Fe-18%Cr have one linear positive slope up to 0.4V_{sce}, on the other hand, alloys higher than the 25%Cr have another linear positive in R4 region.

Fig. 2 is the Mott-Schottky plot showing the $1/C^2$ vs. E of Fe oxide (R3) in the passive films formed on Fe-25%Cr alloys by using capacitance measurement, starting from film formation potential (-0.2V_{sce} to 0.8V_{sce})

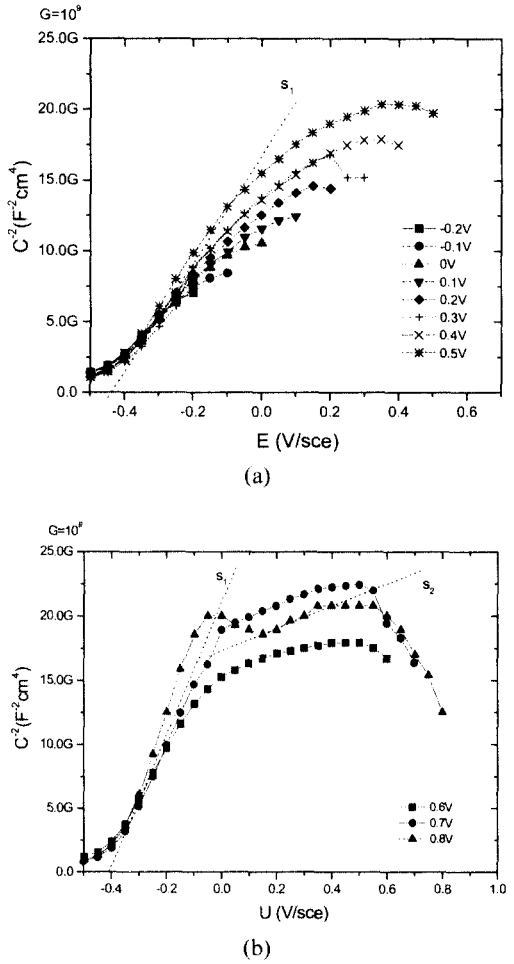

Fig. 2. Mott-Schottky plots for the passive film formed on Fe-20Cr at different film formation potentials in deaerated pH 9.2 buffer solution.

to -0.5V_{sce} in the cathodic direction. Passive films formed at potentials of -0.2V_{sce} to 0.5V_{sce} show one linear positive slope (Fig. 2(a)), while passive films formed at potentials

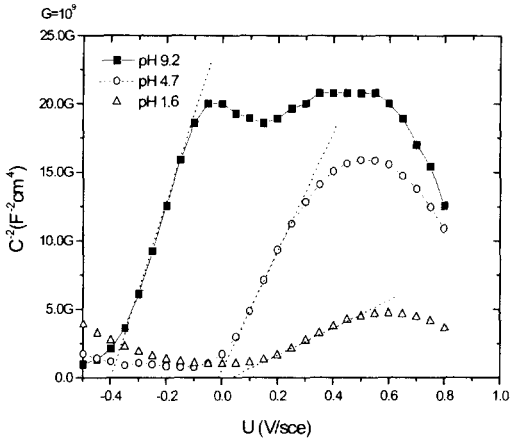

(a)

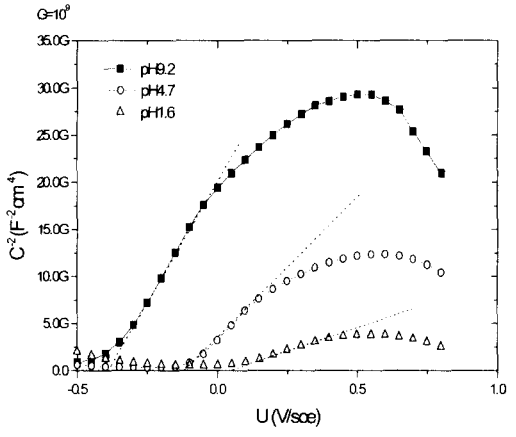

(b)

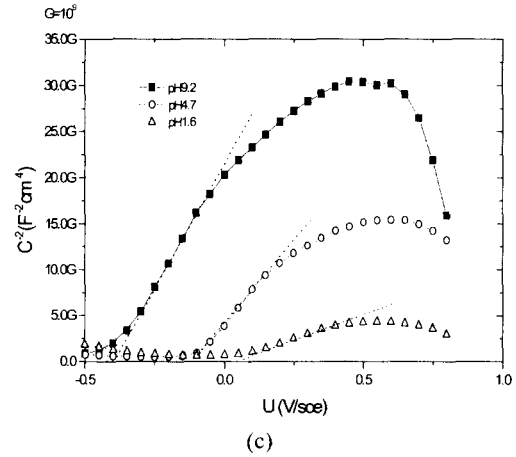

(c)

Fig. 3. Plots of $1/C^2$ vs. the applied potential E for passive filmed at 0.8Vsce on (a) Fe-25%Cr ,(b) Fe-18%Cr, (c)Fe-18%Cr-4%Mo

of $0.6V_{sce}$ to $0.8V_{sce}$ exhibit two linear positive slopes (Fig. 2 (b)). Thus, role of film formation potentials seems to be very similar to that of Cr content.

Fig. 3 shows Mott-Schottky plots of the passive films formed on Fe-25%Cr, Fe-18%Cr and Fe-18%Cr-4%Mo

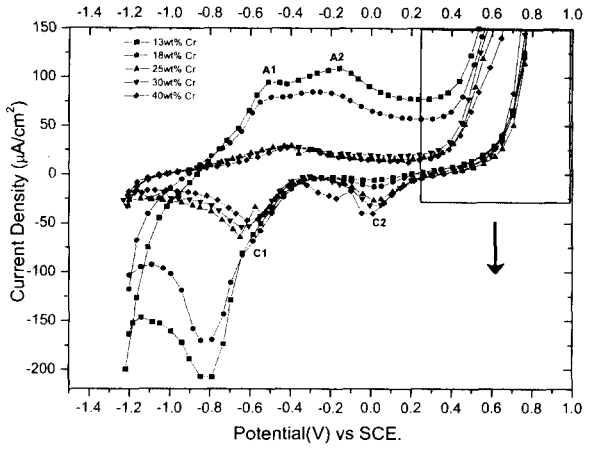

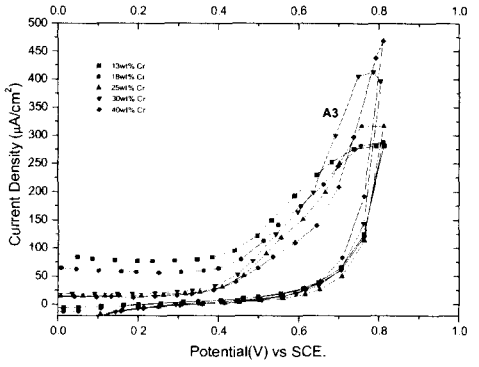

Fig. 4. Cyclic voltammogram obtained for various Fe-Cr alloys at film formation potential of 0.8Vsce in deaerated pH 9.2 buffer solution.

alloys for 2 hour at film formation potential of $0.8V_{sce}$. Three different pH solutions such as pH 9.2, 4.7 and 1.6 were chosen. The increases in capacitance value of alloys were observed with decreasing pH. The change of positive slope was bigger in acidic solution than in neutral and alkali solutions.

3.2 Cyclic voltammetry results

Fig. 4 shows the cyclic voltammogram of passive films formed on Fe-Cr alloys with various Cr contents at film formation potential of $0.8V_{sce}$. Peaks A1 and A2 were related to the oxidations of Fe to Fe^{2+} and of Fe_3O_4 to Fe_2O_3, respectively. Peak A3 is associated with the oxidation of Cr_2O_3 to CrO_4^{2-}. Peaks C1 and C2 were associated with the reduction of Fe oxide to Fe and of Cr^{6+} to Cr^{3+}, respectively, in the cathodic scan. For Fe-Cr alloys higher than 25wt% Cr, peaks A1 and A2 combined together to one peak and peak current density decreased. Subsequently, peak C1 shifted from $-0.8V_{sce}$ to $-0.6V_{sce}$, showing the decreased peak current density. The heights of peak A3 and C2 related to oxidation and reduction of Cr^{6+}/Cr^{3+} increased with increasing Cr content.

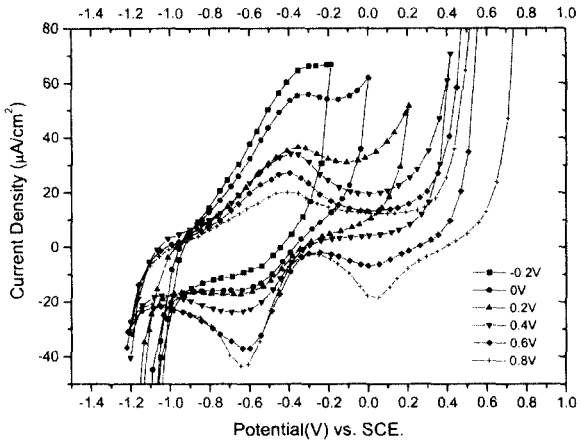

Fig. 5. Cyclic voltammogram obtained for various Fe-25wt%Cr alloy at different film formation potential in deaerated pH 9.2 buffer solution.

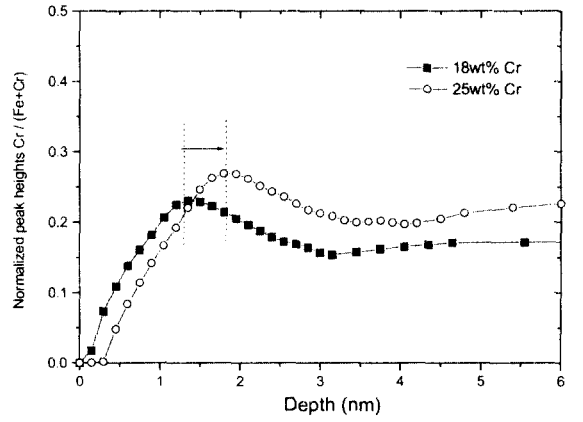

Fig. 6. Auger depth profile of the oxide film formed Fe-18wt%Cr and Fe-25wt%Cr for 2hours at film formation potential of 0.8Vsce in deaerated pH9.2 buffer solution.

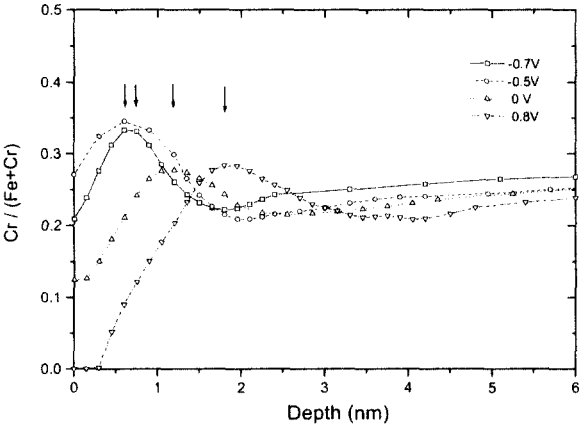

Fig. 7. Auger depth profile of the oxide film formed Fe-25wt%Cr for 2hours at various film formation potential of 0.8Vsce in deaerated pH9.2 buffer solution.

Fig. 5 is the cyclic voltammogram obtained from Fe-25%Cr alloys with passive films formed at various film formation potentials in deaerated pH 9.2 buffer solution. Initial scan was in the andic direction from -1.2V_{sce} to film formation potentials, followed by scaning from film formation potential to -1.2V_{sce} in the cathodic direction. As film formation potential increased, the anodic current density decreased. In case of film formation potentials higher than 0.6V_{sce}, the cathodic current peak due to reduction of Cr^{6+} to Cr^{3+} was observed around 0Vsce.

3.3 Auger electron spectroscopy (AES) results.

Fig. 6 shows the AES result of Cr/(Cr+Fe) in-depth profiles obtained from the passive films formed on Fe-18%Cr and Fe-25%Cr for 2 hour at film formation potential of 0.8V_{sce} in deaerated pH 9.2 buffer solution. As Cr content increased, peak values shifted into the inner side of the film. Fig. 7 presents the results of Cr/(Cr+Fe) in-depth profiles of passive films formed on Fe-25%Cr for 2 hour at film formation potentials of -0.7V_{sce}, -0.5V_{sce}, 0V_{sce} and 0.8V_{sce} in deaerated pH 9.2 buffer solution. As film formation potential increases, peak value goes from the vicinities of solution/film interface to increase to film/metal interface. The thickness of passive film seems to increase with increasing Cr content and film formation potential.

4. Discussion.

4.1 Effect of Cr on electronic behaviors of passive films.

Assuming that the capacitance of the space charge layer is much less than of the Helmholtz layer, the measured capacitance is regarded as the capacitance of space charge layer. The Mott-Schottky equations as follows:[4)-5),8)-12),15)]

$$\frac{1}{C_{sc}^2} = \frac{2}{\varepsilon\varepsilon_o e N_D}\left(E - E_{fb} - \frac{kT}{e}\right) \quad \text{for n-type semiconductor (1a)}$$

$$\frac{1}{C_{sc}^2} = -\frac{2}{\varepsilon\varepsilon_o e N_A}\left(E - E_{fb} - \frac{kT}{e}\right) \quad \text{for p-type semiconductor (1b)}$$

Where ε is the dielectric constant of passive film, taken as 12,[10),16)] ε_o is the permittivity of free space (8.854×10^{-14} F/cm), e is electron charge, N_D and N_A are the donor and acceptor densities, respectively, E_{fb} is the flat band potential, k is the Boltzman constant and T is the absolute temperature. N_D and N_A can be determined from the slopes of the Mott-Schottky plot.

Fig. 8 shows donor and acceptor densities of passive films formed on Fe-Cr alloys in pH 9.2 buffer solution.

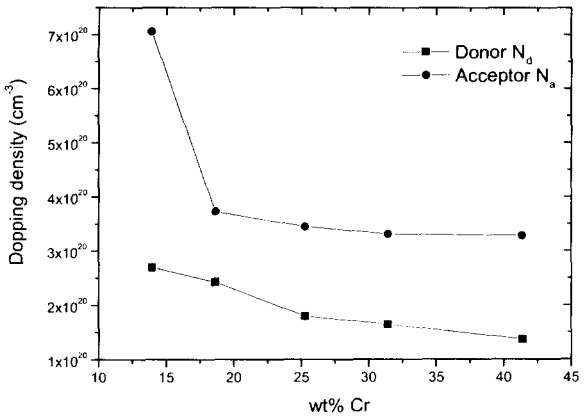

Fig. 8. Doping densities of the passive films formed on Fe-Cr alloys at film formation potential of 0.8Vsce in deaerated pH9.2 buffer solution.

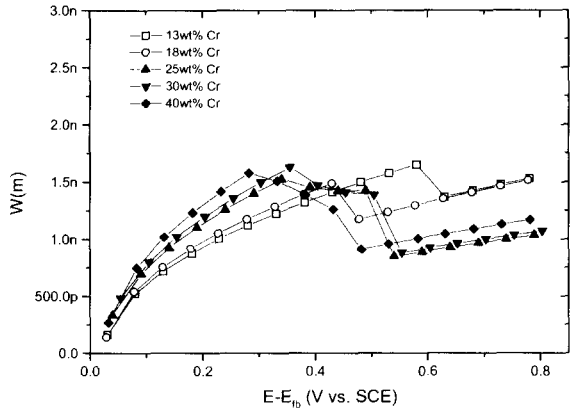

Fig. 9. Thickness variation of space charge region with increasing E-E_{fb}

Film formation potential was $0.8V_{sce}$. The orders of magnitude of doping densities were 10^{20}-10^{21} cm^{-3}, which are comparable to those calculated by some researchers.[4),8),10),13)] Such high doping densities indicate the highly disordered nature of passive film. As Cr content increased, acceptor and donor densities decreased. The remarkable decrease in donor density was observed with the change of Cr content from the below 18%Cr to the above 18%Cr.

The thickness of the space charge layer of n-type semiconductor formed in the region of applied potentials higher than the flat band potential (W) can be calculated by the following equation.[5),14)]

$$W = [\frac{2\varepsilon\varepsilon_o}{eN_D}(E - E_{fb} - \frac{kT}{e})]^{1/2} \quad (2)$$

Fig. 9 shows the influence of Cr content on the thickness of space charge layer as function of E-E_{fb} by using equation (2) (R3 region in Fig. 1). The thickness of space charge layer increased with the increase in Cr content. Xuan et al.[5)] suggested that the higher thickness of space charge layer, the higher resistance of pitting corrosion. It seems that space charge layer plays an effective barrier to the flow of carriers, such as electrons and holes, from semiconductor to electrolyte. However, for E-E_{fb} higher than 0.3V (R4 region in Fig. 1), it seems that Eq(2) did not work to calculate the space charge layer thickness, due to the complicated characteristics of R4 region.

4.2 The effect of film formation potential on electronic behavior of passive film

Based on experimental results by cyclic voltammentry and AES analysis, it is noted that the increase in film formation potential give rise to the increase in the thickness of the passive film, because the maximum of Cr/(Fe+Cr) ratio shifts to the inner region of passive film (Fig. 7). As shown in Fig. 2, Mott-Schottky plot for passive film formed on Fe-25%Cr alloy in film formation potential range above 0.6Vsce is quite different from that below $0.6V_{sce}$. Based on cyclic voltammogram results, Cr^{6+} ions may be responsible for this difference, acting as the deep donor at the film formation potential above $0.6V_{sce}$. The reason is that above $0.6V_{sce}$, the oxidation reaction such as $Cr^{3+} \rightarrow Cr^{6+} + 3e^-$ may occur.

The shallow donor (N_{D1}) and the deep donor (N_{D2}) can be calculated from the slope in Mott-Schottky plot by using the following equation.[13),15)]

$$S_1 = \frac{2}{\varepsilon\varepsilon_o N_{D1}} \quad (3a)$$

$$S_2 = \frac{2}{\varepsilon\varepsilon_o (N_{D1} + N_{D2})} \quad (3b)$$

S_1 and S_2 are positive slopes of R3 and R4 regions shown in Fig. 1. Fig. 10 shows the change of donor densities as a function of film formation potential. Donor densities, shallow donor (N_{D1}), deep donor (N_{D2}) and N_{D1}+ N_{D2}, decreased with increasing film formation potential.

The passive film formed at film formation potentials of $0.6V_{sce}$ and $0.8V_{sce}$ showed increase in reduction peak of Cr^{6+}/Cr^{3+} in cyclic voltammogram and the two linear positive slopes (in R4) of Mott-Schottky plot. These results may be associated with the presence of Cr^{6+} ions in the passive film formed on $0.6V_{sce}$. Because $Cr^{3+} \rightarrow Cr^{6+} + 3e^-$ reaction may occur, the Cr^{6+} are stable in film formed at potentials of $0.6V_{sce}$ and $0.8V_{sce}$.

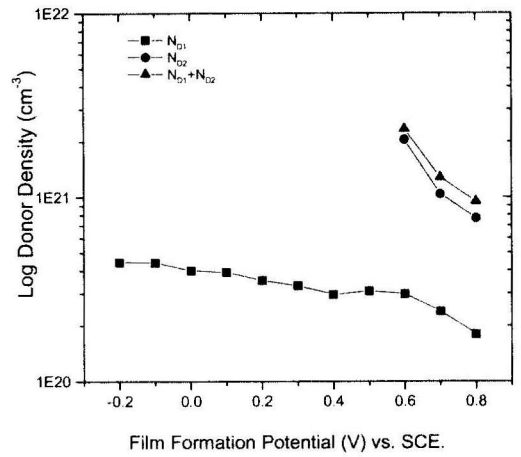

Fig. 10. Variation of donor densities of shallow level(ND_1), deep level(ND_2) and total (ND_1+ND_2) with increasing film formation potential in deaerated pH 9.2 buffer solution.

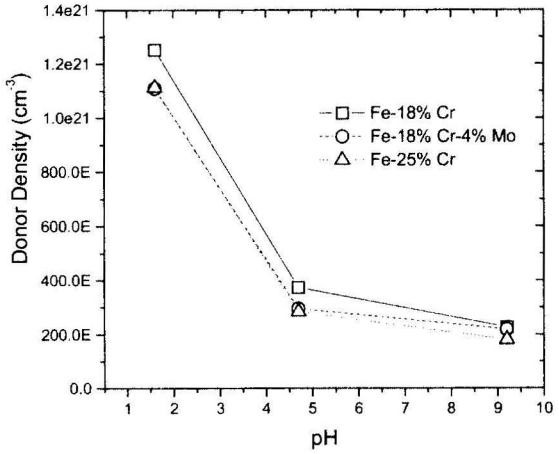

Fig. 11. Variation of doping densities of the passive films formed on Fe-18%Cr, Fe-18%Cr-4%Mo and Fe-25%Cr Alloys with increasing pH.

4.3 The effects of pH and Mo on electronic behavior of passive film.

Fig. 11 shows the donor densities of the passive films formed on Fe-18%, Fe-25%Cr and Fe-18%Cr-4%Mo alloys. With decreasing pH, donor densities of every alloy increased. Especially, with decreasing pH 4.7 to pH 1.6, sudden rise of donor density was observed because of the more corrosive environment. In pH 9.2 solution, the addition to 4%Mo to Fe-18%Cr have little influence on the donor density. While in acidic solution of pH 1.6, Mo plays some role in the decreasing in donor density. Since the decrease in donor density is related to the decrease in the number of defects, Mo seems to assist in improving corrosion resistance. In terms of donor density, Fe-18%Cr-4%Mo alloy may be comparable to Fe-25%Cr alloy.

5. Conclusions

1) As Cr content and film formation potential increased, donor and acceptor decreased. The decrease in doping density results in the decrease in defects, causing the higher resistance to corrosion.

2) As Cr content and film formation potential increased, thickness of space charge layer and passive film increased.

3) Based on cyclic voltammogram and Mott-Schottky plot of Fe-Cr alloys, Cr^{6+} ion may be responsible for deep donors.

4) Mo plays some role in decreasing donor density in acidic solution while the addition of Mo to Fe-Cr alloy have little influence on the change of donor density in alkali solution.

Acknowledgement

Authors gratefully acknowledge the financial support from Korea Science and Engineering Foundation (KOSEF) under the contraction number of 2000-1-301-012-3.

References

1. G. Bianchi, A. Cerquetti, F. Mazza, and S. Torchio, *Corro. Sci.*, **12**, 495 (1972).
2. E. K. Oshe and I. L. Rozenfeld, *Z. Metallov.*, **5**, 524 (1969),
3. P. Schmuki and H. Bohni, *J. Electrochem. Soc.*, **139**, 7 (1992).
4. M. Da Cunha Belo, B. Rondot, C. Compere, M. F. Montemor, A. M .P Simoes, and M. G. S. Ferreira, *Corro. Sci.*, **40**, 481 (1998).
5. Q. Le Xuan, B. Rondot, and M. Da Cunha Belo, *Ann. Chim. Sci. Mat*, **23**, 607 (1998).
6. L. M. Peter, *Ber. Bunsenges. Phys. Chem.*, **91**, 419 (1987).
7. T. D. Burleigh, *Corrosion*, **45**, 464 (1989).
8. A. D. Paola, *Electrochim. Acta*, **34**, 203 (1989).
9. A. D. Paola, D. Shukla, and U. Stimming, *Electrochim. Acta*, **36**, 345 (1991).
10. N. E. Hakiki, S. Boudin, B. Rondot, and M. Da Chunha Belo, *Corros. Sci.*, **37**, 1809 (1995).
11. N. E. Hakiki, M. Da Cunha Belo, A. M. P. Simoes, and M. G. S. Ferreira, *J. Electrochem. Soc.*, **145**, 3821 (1998).
12. N. E. Hakiki, M. F. Montemor, M. G. S. Ferreira, and M. Da Cunha Belo, *Corros. Sci.*, **42**, 687 (2000).
13. A. M. P. Simoes, M. G. S. Ferrira, B. Rondot, and M. Cunha Belo, *J. Electrochem. Soc.*, **137**, 82 (1990).
14. J. B. Lee and D. H. Ham, *J. Korean Electrochem. Soc.*, **2**, 195 (1999).
15. Y. F. Cheng and J. L. Luo, *Electrochim. Acta*, **44**, 2947 (1999).
16. B. Lovrecek and J. Sefaja, *Electrochim. Acta*, **17**, 1151 (1972).